Int. J. Heat Mass Transfer. Vol. 33, No. 5, pp. 931–942, 1990
Printed in Great Britain

0017-9310/90 $3.00+0.00

Heat transfer due to buoyancy in a partially divided square box

S. ACHARYA and R. JETLI
Mechanical Engineering Department, Louisiana State University, Baton Rouge, LA 70803, U.S.A.

(*Received* 3 *November* 1988 *and in final form* 26 *July* 1989)

Abstract—The heat transfer and flow patterns in a partially divided square box have been studied numerically. The partial divider is thin, poorly conducting and projecting upwards from the floor of the enclosure. Three divider positions and divider heights (enclosure apertures) are considered. Results obtained are compared with published computational and experimental studies and provide a unifying picture of flow and heat transfer in partially divided enclosures. The thermal stratification between the divider and the cold wall is found to play a key role. At lower Rayleigh numbers (10^5–10^6) the flow is weak in this stratified region and a tendency for flow separation behind the divider is noted. At higher Rayleigh numbers ($> 10^9$) the stratification is significant in this region and causes the flow to detach directly from the cold wall causing a separation in front of the divider. The enclosure heat transfer is strongly influenced by the aperture ratio A_p ($Nu \approx A_p^{0.462}$). However, the divider position has a rather small effect on the overall heat transfer from the enclosure.

INTRODUCTION

NATURAL CONVECTION in an enclosure with a partial vertical divider has received a considerable degree of recent interest. Enclosures with a single divider projecting vertically upwards or vertically downwards, and enclosures with two dividers, one projecting upwards and the other downwards, have both been studied.

Duxbury [1] has conducted an experimental study in a centrally divided air-filled enclosure. Rayleigh numbers studied were in the range of 8×10^4–5×10^6. A tendency for the flow to detach behind the divider was noted. Winters [2] performed a companion numerical study with assumed adiabatic end walls and obtained flow patterns that were qualitatively similar with flow separation behind the divider. Nansteel and Greif [3, 4] conducted an experimental study at higher Rayleigh numbers (10^{10}–10^{11}) and an aspect ratio of 1/2. Water was the working fluid, and the horizontal end walls were made of plexiglass. Measurements seem to indicate that the end walls were adiabatic. In direct contrast to the studies of Duxbury [1] and Winters [2] where flow separation was noted behind the divider, Nansteel and Greif [3, 4] observed the flow separation to occur in front of the divider. Lin and Bejan [5] carried out a similar high Rayleigh number experimental study with water as the working fluid and for an enclosure aspect ratio of 1/2. Flow patterns similar to those observed by Nansteel and Greif [3, 4] were noted, but the Nusselt number results obtained were considerably lower than Nansteel and Greif's data. Winters [6] has recently conducted a numerical study of natural convection in a partially divided enclosure with adiabatic end walls. Rayleigh numbers studied were in the range of 10^6–10^{11}. At Rayleigh numbers around 10^6 the flow in front of the divider was considerably weaker than that behind it. At higher Rayleigh numbers, as observed by Nansteel and Greif [3, 4] and Lin and Bejan [5], the flow separated in front of the divider. More recently Kirkpatrick *et al.* [7] and Zimmerman and Acharya [8] have performed a numerical study of natural convection of air in a vertical enclosure with a centrally located divider. Results were obtained at lower Rayleigh numbers, and no flow separation in front of the partial divider was noted. The heat transfer results of Kirkpatrick *et al.* [7] agreed to within 10% with Nansteel and Greif's data, but differed substantially from Lin and Bejan's values. On the other hand, the predictions of Zimmerman and Acharya [8] compared well with the measurements of Lin and Bejan.

In addition to the aforementioned studies on an enclosure with a single divider, a number of additional studies have been undertaken on natural convection in an enclosure with two dividers, one projecting upwards and the other downwards. These include the experimental studies of Probert and Ward [9] and Janikowski *et al.* [10] who determined the heat transfer across high aspect ratio enclosures with either in-line or offset dividers. Bajorek and Lloyd [11] undertook an experimental study and Chang [12] performed a companion numerical study for natural convection in a divided square enclosure. Zimmerman and Acharya [13] and Jetli and co-workers [14–16] have performed a series of calculations for heat transfer in an enclosure with in-line and offset dividers and with adiabatic or conducting end walls. Predictions were compared with the experimental data of Bajorek and Lloyd [11]. Quantitative results were in good agreement only for the predictions obtained with assumed conducting end walls. This is consistent with the

NOMENCLATURE

A_p	aperture ratio, $(H-h)/L$
c_p	specific heat of fluid
d	thickness of the divider
g	acceleration due to gravity
H	enclosure height
h	divider height
k	thermal conductivity of air
k_d	thermal conductivity of divider
k_r	conductivity ratio, k_d/k
L	enclosure width
$Nu, \overline{Nu}$	Nusselt number (hH/k), and average Nusselt number
p	thermodynamic pressure
P	dimensionless pressure
Pr	Prandtl number, $\mu c_p/k$
Ra	Rayleigh number, $g\beta(T_h - T_c)H^3/\nu\alpha$
T	dimensional temperature
T_c, T_h	cold wall and hot wall temperatures
T_0	reference temperature, $(T_c + T_h)/2$
u, U	dimensional and dimensionless velocity in the x-direction
v, V	dimensional and dimensionless velocity in the y-direction
x, X	dimensional and dimensionless coordinate along the horizontal direction
x_d	dimensional x-location of the divider
y, Y	dimensional and dimensionless coordinate along the vertical direction.

Greek symbols

α	thermal diffusivity
β	volume expansion coefficient at constant pressure
θ	dimensionless temperature
θ_d	dimensionless temperature in divider
ν	kinematic viscosity
ρ	density
ψ	stream function
ψ_{max}	maximum stream function.

measurements of Krane and Jesse [17] and El Sherbiny *et al.* [18], who noted that with air as the working fluid the horizontal end walls behave more like a perfectly conducting material rather than an insulating material. This is true even if the end walls are made up of a poorly conducting material such as plexiglass. If, however, the working fluid has a higher conductivity, such as water, then plexiglass end walls are better described by adiabatic conditions as observed in the experiments of Nansteel and Greif [3, 4]. Thus, in determining the appropriate conditions along the end wall, the ratio of the thermal conductivity of the fluid to that of the end wall is the important parameter. With air as the working fluid, the end walls are better described by perfectly conducting end wall conditions.

In this paper, natural convection of air in a square enclosure with a single partial divider is considered. In view of the arguments in the previous paragraph, perfectly conducting conditions should be assumed along the end walls. Yet, for an enclosure with a single divider, all reported studies assume adiabatic end walls. The only exception is the study of Zimmerman and Acharya [8], where only centrally located dividers were considered. The present paper extends the study of Zimmerman and Acharya [8] and examines the effect of the divider position (x_d) and divider height (h) or enclosure aperture ($h_{ap} = H-h$) on the enclosure heat transfer and flow patterns. Three divider positions and divider heights (or enclosure aperture) are considered (Fig. 1). A second objective of the paper is to provide a more unifying picture of the various observations on heat transfer and flow patterns in an enclosure with a single vertical divider. As noted earlier, there are several inconsistencies in the reported literature regarding quantitative heat transfer data, and more importantly, whether the flow separates in front of the divider or behind it. Some of these inconsistencies are addressed in this paper.

GOVERNING EQUATIONS

The flow is assumed to be laminar, steady and two-dimensional in a box whose z-dimension is much larger than the x- and y-dimensions. Nansteel and Greif's experiments confirm these assumptions even for Rayleigh numbers as high as 10^9–10^{10}. This is because the presence of partial dividers induces thermal stratifications that have a stabilizing effect on the flow and inhibit transition to turbulence. For the Rayleigh numbers of interest in this study, these assumptions have also been shown to be valid for undivided enclosures [19].

For property variations, the Boussinesq approximation is invoked according to which all properties are assumed to be constant, except the density appearing in the body force term, which is expressed as

$$\rho = \rho_0[1 - \beta(T - T_0)]. \quad (1)$$

For small and moderate temperature differences, the Boussinesq assumption has been shown to be valid both experimentally and computationally [13, 20]. In addition to the Boussinesq assumption, for the moderate temperature differences considered in this study radiation effects have been neglected.

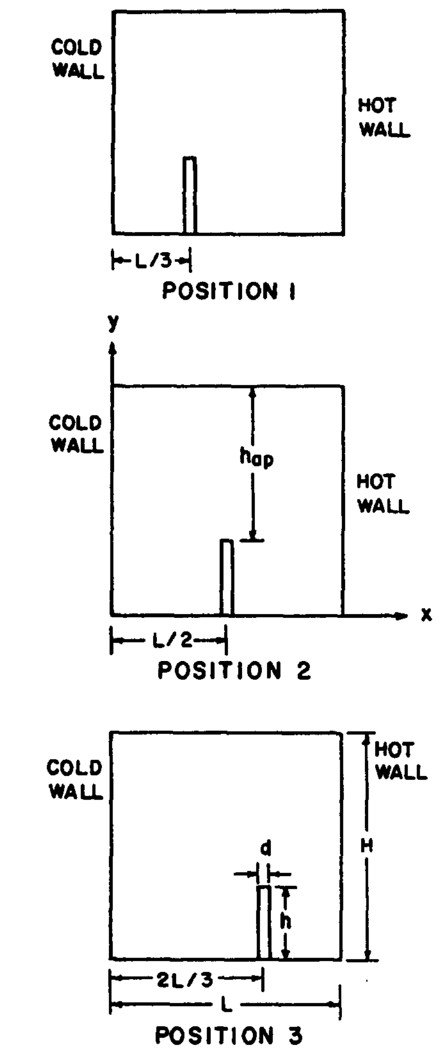

FIG. 1. Schematic of the partially divided enclosure.

If the following dimensionless variables are introduced

$$X = x/L, \quad Y = y/L \tag{2}$$

$$U = u/(\nu/L), \quad V = v/(\nu/L),$$

$$P = (p+\rho g y)/\{\rho/(\nu/L)^2\} \tag{3}$$

$$\theta = (T-T_0)/(T_h-T_0) \tag{4}$$

the non-dimensional mass, momentum and energy equations become

$$\partial U/\partial X + \partial V/\partial Y = 0 \tag{5}$$

$$U\partial U/\partial X + V\partial U/\partial Y = -\partial P/\partial X + (\partial^2 U/\partial X^2 + \partial^2 U/\partial Y^2) \tag{6}$$

$$U\partial V/\partial X + V\partial V/\partial Y = -\partial P/\partial Y + (\partial^2 V/\partial X^2 + \partial^2 V/\partial Y^2) + Ra\cdot\theta/Pr \tag{7}$$

$$U\partial\theta/\partial X + V\partial\theta/\partial Y = (\partial^2\theta/\partial X^2 + \partial^2\theta/\partial Y^2)/Pr. \tag{8}$$

In the divider region, since the velocity field is zero, the governing equations reduce to the Laplace equation and the non-dimensional temperature distribution can be expressed as

$$(k_r/Pr)(\partial^2\theta_d/\partial X^2 + \partial^2\theta_d/\partial Y^2) = 0 \tag{9}$$

where k_r is the ratio between the thermal conductivity of the divider and the convective fluid and θ_d is the non-dimensional temperature in the divider.

The energy balance at the divider–air interface requires that

$$\frac{1}{Pr}\left(-\frac{\partial\theta}{\partial n}\right)_{\text{interface}} = \frac{k_r}{Pr}\left(-\frac{\partial\theta_d}{\partial n}\right)_{\text{interface}} \tag{10}$$

where 'n' denotes the normal to the surface at the divider–air interface.

The problem is solved using the no-slip boundary conditions along the walls. The hot and cold walls are maintained at non-dimensional temperatures of 0.5 and −0.5, respectively. The Prandtl number is assumed to be 0.71. As noted earlier, the horizontal end walls should be assumed to be perfectly conducting if air is the working fluid. This has been clearly demonstrated by Zimmerman and Acharya [13] for a partially divided enclosure and by El Sherbiny *et al.* [18] and Zimmerman and Acharya [20] for an undivided enclosure.

SOLUTION PROCEDURE

The governing differential equations for the problem are equations (5)–(9), and these should be solved subject to the interface condition (equation (10)) and the relevant boundary conditions. This is done by a control volume based finite difference procedure described in detail by Patankar [21].

In this method, the solution domain is divided into a number of control volumes, each associated with a centrally located grid point. To avoid a checkerboard pressure and velocity field, a staggered grid is used for the velocity. The governing differential equations are expressed in an integral form over each control volume, and profile approximations are assumed in each coordinate direction. This reduces the differential equation to a system of algebraic equations which are then solved iteratively using a line by line Thomas algorithm. In this paper, power law profile approximations, recommended by Patankar [21], are made in each coordinate direction. Pressure–velocity coupling is resolved through a prediction–correction approach called SIMPLER (semi implicit method for pressure linked equations revised).

The presence of the divider in the calculation domain is accounted for by a strategy suggested by Patankar [22], in which equations (5)–(8) are solved in the complete domain, with the divider characterized by a very high viscosity (10^{30}) and the dimensionless divider conductivity (k_r/Pr). Because of the high viscosity and the no-slip boundary conditions the velocities in the divider region are nearly zero (10^{-30}), and therefore the energy equation (equation (8)) in the divider region reduces to the appropriate heat conduction equation (equation (9)). Energy balance at the baffle–air interface is ensured by arranging the control volume faces to coincide with the divider interface. Since a conservative numerical scheme is being used, energy into and out of the divider interface must be equal to each other, thus satisfying equation (10).

NUMERICAL ACCURACY

To determine a suitable grid size, the computed profiles of velocity, temperature, and the local Nusselt number were compared for a number of grid sizes. A final grid size of 48×42 grid points was chosen for this study. The grid points were packed along the solid boundaries to provide a better resolution of the large gradients expected in these regions. Comparison of the solution from the 48×42 grid chosen in this paper with the solution on an 80×72 grid revealed that the maximum differences were less than 2% in the peak Nusselt number value and less than 1.6% in the peak mid-height horizontal velocity. Conservation of mass, momentum and energy was found to be satisfied to within 1% in each control volume. Typical computing times on an IBM 3084 for the 48×42 grid chosen were of the order of 20–30 min.

RESULTS AND DISCUSSION

The three divider locations considered are $x/L = 1/3$, $1/2$ and $2/3$ from the cold wall. The enclosure aperture opening ratio ($A_p = h_{ap}/H$) is varied from $A_p = 1/3$, $1/2$ to $2/3$, for all three divider positions, except for the centrally located divider, where two additional aperture ratios of $A_p = 1$ (no divider) and 0 (complete divider) are studied. The divider thickness (d) and the thermal conductivity ratio (k_r) were kept at $L/20$ and 2 respectively to simulate a thin, poorly conducting divider. The Rayleigh number values studied were in the range $Ra = 10^4$ to 3.55×10^5.

The results are presented in two sections. The first section highlights the effect of aperture ratio on a single centrally located divider, while the next section studies the effect of divider position.

Effect of aperture ratio in an enclosure with a centrally located divider

At the lowest Rayleigh number ($Ra = 10^4$) studied (no streamline or isotherm plots presented), a relatively weak convective flow exists in the cavity and the flow patterns and the temperature distributions tend to be symmetrical on either side of the divider. At $Ra = 10^5$ and 3.55×10^5, as the aperture opening is reduced, a distinctly weaker flow is observed between the divider and the cold wall (Fig. 2), compared to the region between the divider and the hot wall. The colder air tends to stagnate in the lower left hand section of the cavity between the divider and the cold wall, resulting in a thermally stratified region and thus preventing the penetration of the warmer fluid from the cavity right hand section. Flow separation behind the divider is noted at $A_p = 2/3$. For $A_p = 0$ (complete divider) the asymmetry on either side of the divider, expectedly, disappears.

An earlier study by Nansteel and Greif [3, 4] studied the effect of varying the aperture ratios in a water-filled enclosure with a single centrally located divider projecting downwards. Rayleigh numbers were in the range of $2.3 \times 10^{10} \leqslant Ra \leqslant 1.1 \times 10^{11}$. While comparing the results of Nansteel and Greif [3, 4] with Duxbury [1] (for a similar divider configuration but with air as the working fluid and Rayleigh numbers in the range of $Ra \cong 10^6$), distinct differences were found. The two main differences were that Nansteel and Greif [3, 4] observed flow recirculation between the hot wall and the top divider, with flow separating off the hot wall in front of the divider. This effect was absent in Duxbury's [1] experiments. Duxbury observed flow separation behind the top divider towards the cold wall, a result contrary to Nansteel and Greif's. Comparing the results of the present study with the equivalent configurations of the above two studies, distinct similarities are found between Duxbury's results and the present results. No flow separation or separate recirculation is observed between the cold wall and the lower divider. Instead, for $A_p = 2/3$, flow separation is observed behind the lower divider towards the hot wall (Fig. 2). These results confirm the existence of a different flow regime at moderate Rayleigh numbers ($Ra \cong 10^5$–10^7) compared to high Rayleigh numbers ($Ra \cong 10^9$–10^{11}). A recent study by Winters [6] has also shown the distinct transition from the moderate Rayleigh number to the high Rayleigh number regime. Winters studied convective flow in a cavity with the same geometry as Nansteel and Greif [3, 4] in the Rayleigh number range of $10^6 \leqslant Ra \leqslant 10^{11}$. The results of Winters [6] for $Ra = 10^6$ are similar to the present results at $Ra = 3.55 \times 10^5$, showing marked asymmetry in flow, with the flow being stronger between the hot wall and the lower divider. At higher Rayleigh numbers ($Ra \cong 10^{10}$) the flow in Winters' study is similar to that in Nansteel and Greif's experiment, with flow separation along the cold wall and recirculation in the divider–cold wall region.

The results of the present work and the previous studies can be summarized to show the clear existence of three different flow regimes at different Rayleigh number ranges, as illustrated in Fig. 3. At the lower Rayleigh numbers a weak symmetric flow exists in the cavity. At moderate Rayleigh numbers, the flow tends to be asymmetric with stronger flow between the lower divider and the hot wall and possible flow separation behind the divider. Finally, at high Rayleigh numbers,

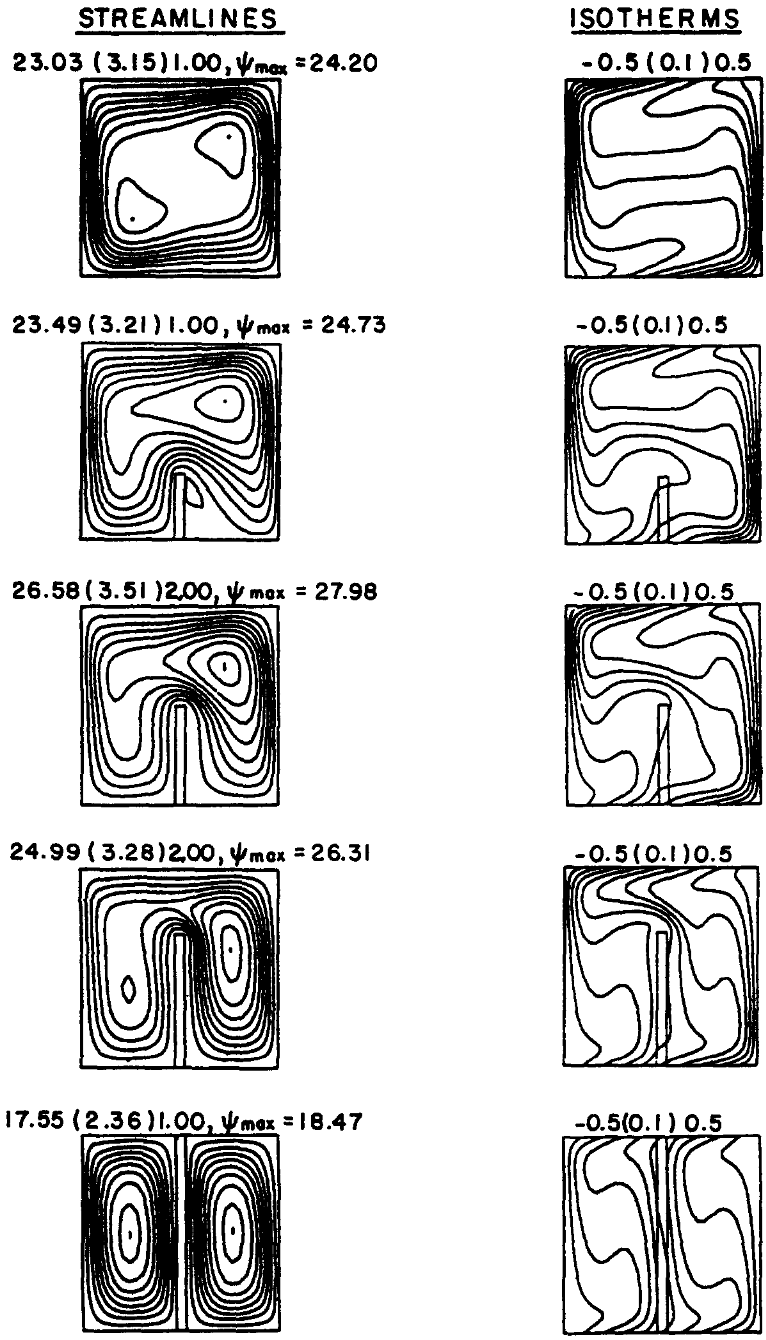

FIG. 2. Streamlines and isotherms for centrally located divider at various aperture ratios ($Ra = 3.55 \times 10^5$).

flow separation along the cold wall leads to a separate recirculation eddy in the divider–cold wall region.

Local Nusselt number variation along the hot and cold side walls are presented in Fig. 4 for $Ra = 3.55 \times 10^5$ and the five aperture ratios studied. Both the hot wall and the cold wall have a sharp peak occurring at the lower and upper sections of the walls, respectively, at the points where the cold and warm flow streams impinge directly onto them. However, in the profiles for the cold wall the sharp peak value is followed by a relatively flatter profile in the lower section due to the flow stratification in that region. The average Nusselt number values for the enclosures (Table 1) show a significant reduction in heat transfer as the aperture opening is reduced. Ratios of the partially divided enclosure Nusselt numbers to those of an open enclosure at the same Rayleigh number reveals that at the higher Rayleigh numbers, the per-

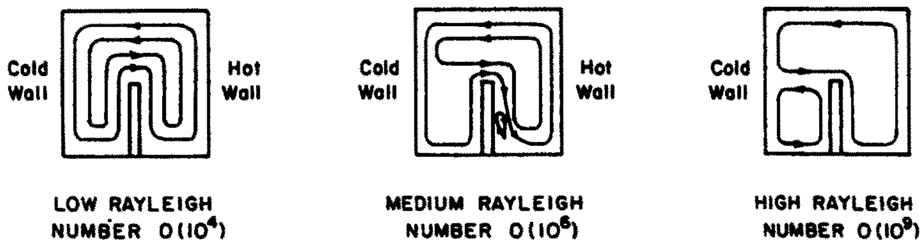

FIG. 3. Schematic of different flow regimes.

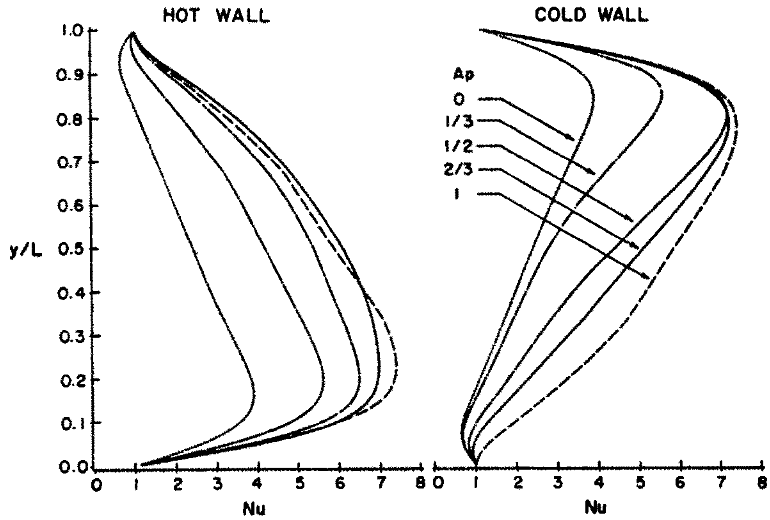

FIG. 4. Local Nusselt number along the vertical side walls for an enclosure with a centrally located divider ($Ra = 3.55 \times 10^5$).

Table 1. Average Nusselt numbers for a partially divided enclosure

Position	Ra	Nu ($A_p = 0$)	Nu ($A_p = 1/3$)	Nu ($A_p = 1/2$)	Nu ($A_p = 2/3$)	Nu ($A_p = 1$)
Position 1	10^4		1.14	1.24	1.47	
	10^5		1.92	2.62	3.02	
	3.55×10^5		3.11	4.02	4.56	
Position 2	10^4	1.05	1.05	1.14	1.39	1.75
	10^5	1.65	1.92	2.72	3.07	3.36
	3.55×10^5	2.25	3.24	4.23	4.66	4.90
Position 3	10^4		1.15	1.21	1.41	
	10^5		1.91	2.50	2.90	
	3.55×10^5		3.38	4.19	4.52	

centage reduction in heat transfer varies from about 5% at $A_p = 2/3$ to 54% at $A_p = 0$.

Correlation of the heat transfer results of the centrally located divider case as a function of A_p and Ra yields the following equation:

$$Nu = 0.091 Ra^{0.318} A_p^{0.462} \tag{11}$$

for $1/3 \leqslant A_p \leqslant 1$, $10^4 \leqslant Ra \leqslant 3.55 \times 10^5$, $Pr = 0.71$.

A recent numerical study by Kirkpatrick *et al.* [7] has presented a correlation for natural convection of air in a partially divided enclosure with an aspect ratio of 1/2. Their correlation is expressed as

$$Nu = 0.881 Ra^{0.316} A_p^{0.309} \tag{12}$$

for $1/8 \leqslant A_p \leqslant 3/4$, $0.9 \times 10^4 \leqslant Ra \leqslant 0.9 \times 10^9$, $Pr = 0.77$.

Comparison of the present study's correlation (equation (11)) with the above equation reveals reasonable agreement between the Rayleigh number exponents but the aperture ratio exponents are different. It may be pointed out that the correlation presented by Nansteel and Greif [3, 4] and Winters [6] for non-conducting dividers has an aperture ratio exponent of 0.473 and 0.437 respectively, which are closer to the results of the present study.

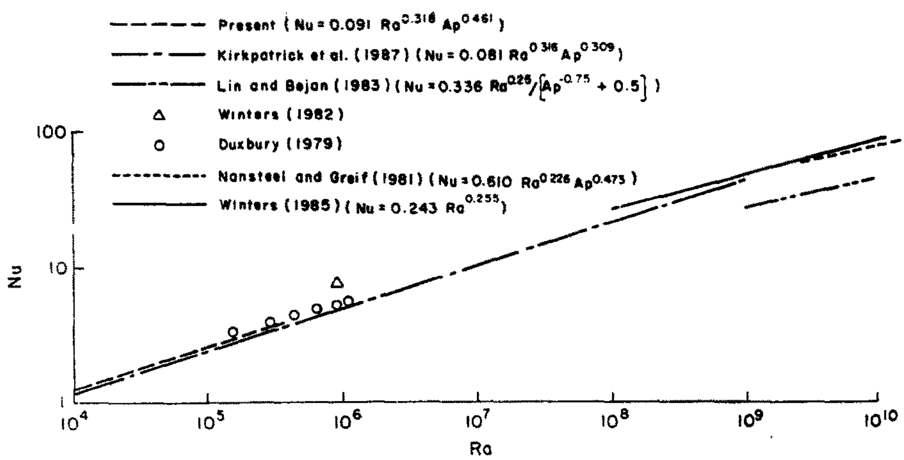

FIG. 5. Summary of heat transfer correlations for centrally divided enclosure at $A_p = 1/2$.

Direct comparison between the present correlation (equation (11)) and the correlations expressed by Nansteel and Greif [3, 4] and Winters [6] cannot be made as they were performed at a larger Prandtl number, a lower aspect ratio ($A = H/L$) of 1/2, and a higher Rayleigh number regime. Figure 5 graphically displays some of these correlations and the present predictions compare well with those reported by others in the same Rayleigh number range. At higher Rayleigh numbers (10^9–10^{10}), the reported correlations appear to have a flatter slope or a smaller exponent of the Rayleigh number. This is perhaps due to the different flow pattern at the higher Rayleigh number regime (Fig. 3).

Effect of divider position

At both the higher Rayleigh numbers studied ($Ra = 10^5$ and 3.55×10^5), there is a distinct thermal stratification in the divider–cold wall regions in position 1, which gradually reduces as the divider is moved towards the hot wall to position 3 (Figs. 6 and 7). This thermally stratified region prevents the bulk of the fluid descending along the cold wall to penetrate the region. Instead, the air tends to flow directly around the divider towards the hot wall. The near stagnant fluid in the divider–cold wall region in position 1 reduces the effective cross flow area in the cavity. On the other hand, as the divider is moved towards the hot wall (position 3), the stratification in the divider–cold wall region is reduced, leading to a larger area for convective flow to take place in the enclosure. Consequently, the stream function values are highest in position 1, lower in position 2, and lowest in position 3.

The only comparable study performed to examine the effect of divider position in an enclosure with a single vertically projecting divider is that of Nansteel and Greif [4]. They observed (at $Ra = 10^{10}$–10^{11}) that there was no qualitative change in the flow as the divider was moved from position 1 to position 3 with the recirculation eddy in the hot wall–downward projecting divider region (equivalent to the cold wall–upward projecting divider region of the present study) merely changing in size to accommodate the geometry as the divider position was moved. However, this is not strictly true at the lower Rayleigh numbers of the present study. Instead of flow separation, a thermally stratified zone develops in the divider–cold wall region, with the stratification decreasing as the divider is moved towards the hot wall. This phenomenon is clearly illustrated in Fig. 7, where there is little flow in the divider–cold wall region in position 1 but a relatively more vigorous flow in position 3.

Figure 8 illustrates temperature profiles in the vertical direction at three cavity cross-sections of $x/L = 1/3$, 1/2, and 2/3, for the three divider positions studied. In position 1, the stratified flow in the divider cold wall region causes the divider (at $x/L = 1/3$) to remain at almost a constant temperature. A sharp temperature gradient exists at a height just above the divider tip, while at $x/L = 1/2$ and 2/3 the profiles are relatively linear. In positions 2 and 3 also, the temperatures in the lower section of the cavity are relatively constant, followed by sharp temperature gradients near the divider tip. The strong influence of the cold stratified air in the lower section of the cavity is evidenced by the fact that the divider tip has a non-dimensional temperature of -0.2, even in position 3 where the divider is nearest to the hot wall.

Local Nusselt number distributions along the isothermal walls are presented in Fig. 9, for the aperture ratio of 1/2. The Nusselt number distribution along the hot wall has two distinct peaks for the divider in position 3. The primary peak is near the bottom of the hot wall with a second peak at a wall height just above the divider tip. The reason for this is that a portion of the cooler air stream rising along the divider impinges directly on the hot wall instead of descending down the divider with the majority flow stream (Fig. 6). This causes the second Nusselt number peak just above the divider tip. This peak is less evident at the higher Rayleigh number as the greater

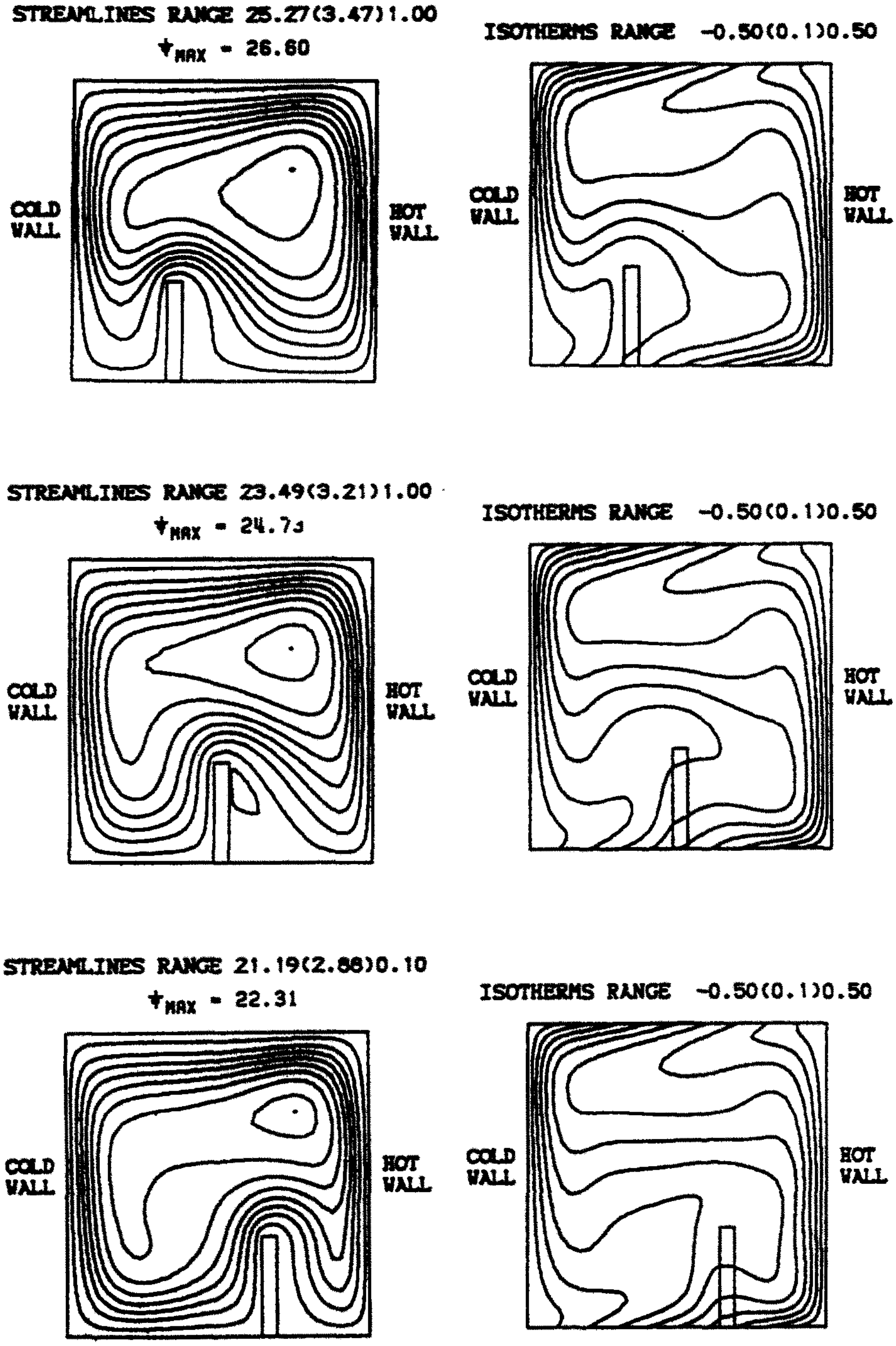

FIG. 6. Streamline and isotherm plots ($A_p = 2/3$, $Ra = 3.55 \times 10^5$).

convective flow increases the strength of the majority flow descending the divider towards the base of the hot wall. A notable difference of the Nusselt number distribution along the cold wall compared to the hot wall is that the cold wall distributions are characterized by strong peaks towards the upper section of the cold wall ($0.6 \leqslant y/H \leqslant 0.9$), followed by relatively linear (position 3) to near constant (position 1) profiles in the lower section of the cavity. This distribution is a consequence of the thermal stratification existing in the lower section of the cavity between the divider and the cold wall (Fig. 7).

The average Nusselt number values at the various divider positions and aperture ratios are summarized in Table 1. As expected, as the aperture ratio is decreased, the amount of heat transfer in the cavity is reduced. The reduction from open or undivided cavity values ranges from 10–20% for $A_p = 2/3$ to 40–50% for $A_p = 1/3$. The effect of divider position on the overall heat transfer rate does not seem to be very

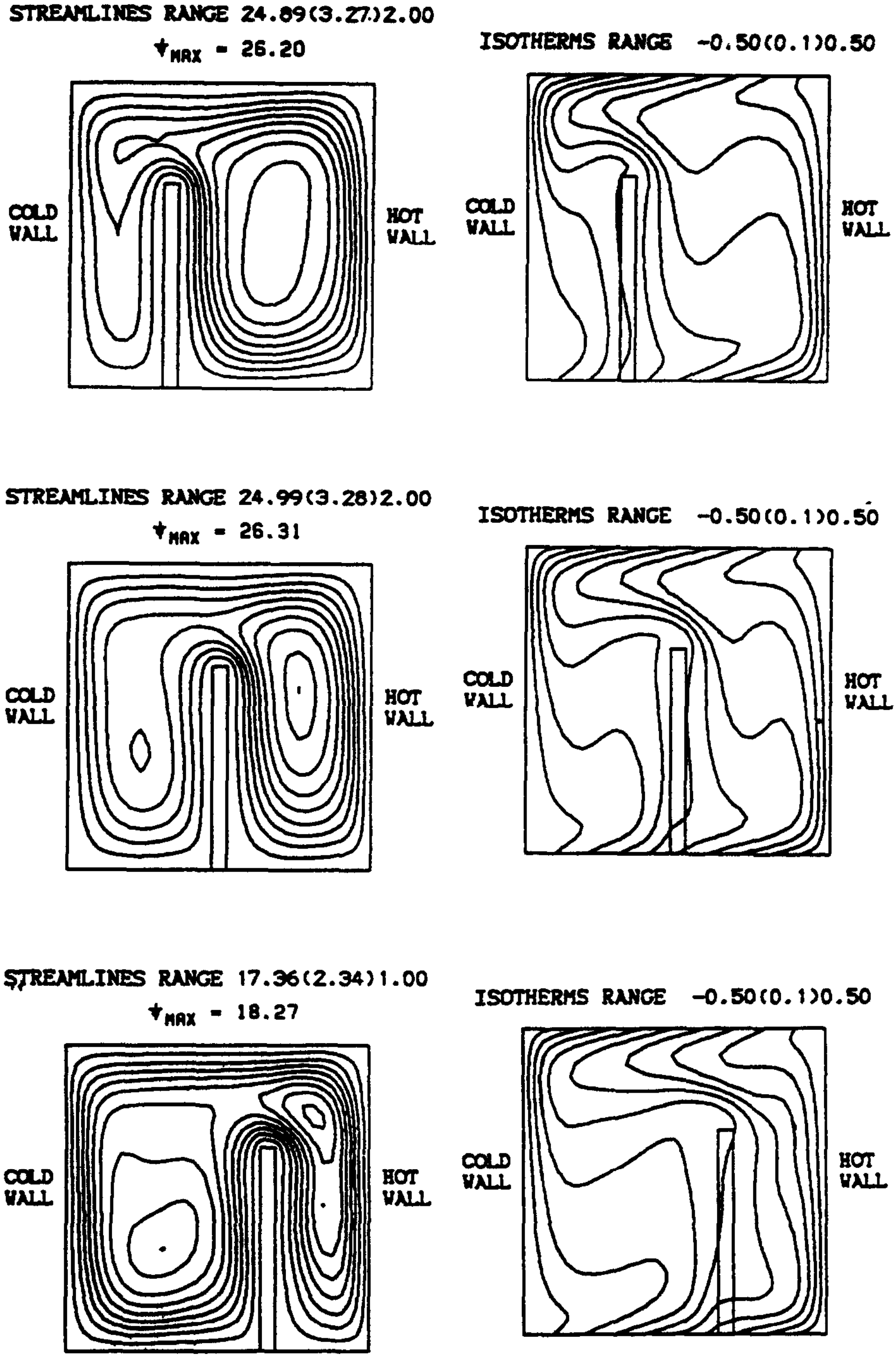

FIG. 7. Streamline and isotherm plots ($A_p = 1/3$, $Ra = 3.55 \times 10^5$).

significant over the parameter range studied. However, several trends do emerge. At higher Rayleigh numbers and aperture ratios of $A_p = 2/3$ and 1/2, position 3 has the lowest heat transfer followed by positions 1 and 2, respectively. In position 3, the cold fluid stream from the cold wall is preheated to a greater degree by the lower end wall and therefore a position of the flow negotiating the divider does not descend along it and is prevented from directly impinging at the base of the hot wall, causing lower temperature gradients and Nusselt numbers in the divider–hot wall region. In position 1, the thermal stratification in the divider–cold wall region reduces the heat transfer in that region considerably. Thus, even though the flow strength is highest in that position, the average heat transfer is lower than in position 2. As the aperture ratio is lowered to 1/3, however, the effect of the thermal stratification in the divider–cold wall region becomes more significant, causing position 1 to have the lowest Nusselt numbers, followed by positions 2 and 3, respectively.

Since the divider position does not have a significant

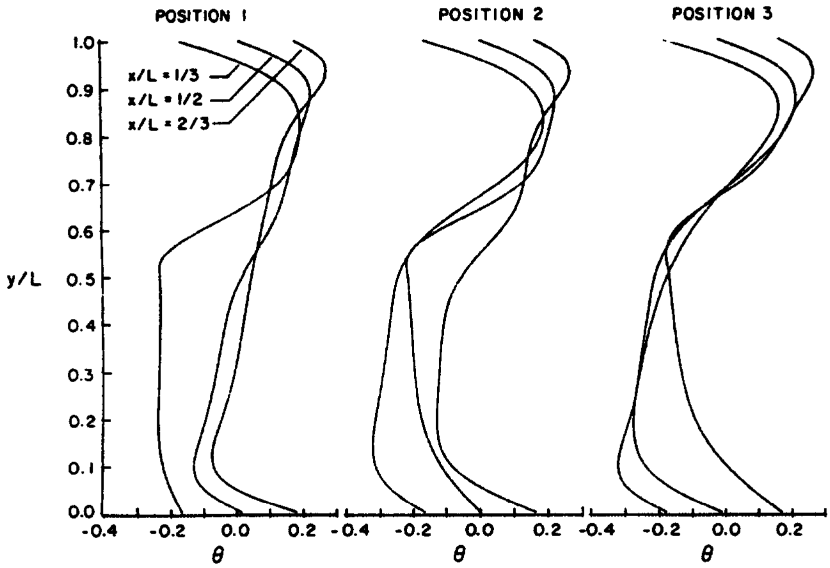

FIG. 8. Vertical temperature profiles at $x/L = 1/3$, $1/2$ and $2/3$ for the three divider positions ($A_p = 1/2$, $Ra = 3.55 \times 10^5$).

effect on the overall cavity heat transfer, the same correlation can be used to predict the heat transfer for all positions. The correlation is expressed by equation (11) presented in the previous section. The root mean square error for the correlation is 6.1%.

CONCLUDING REMARKS

In this paper the influence of divider position and divider height (or enclosure aperture) have been studied for an enclosure with a single divider. The existence of distinctly different Rayleigh number flow regimes is confirmed by comparing the present data with prior published results. At moderate Rayleigh numbers ($Ra \cong 10^5$–10^6) a distinctly asymmetric flow exists with stronger flow in the divider–hot wall region and there is a tendency for flow separation behind the divider. At the higher Rayleigh numbers ($Ra \cong 10^{10}$) flow separation occurs along the cold wall, leading to a separate recirculation eddy between the divider and the cold wall. A correlation expressing the average Nusselt number for the cavity was presented and compared with existing correlations and experimental data. The divider height (or enclosure aperture ratio) has a much stronger effect on the cavity heat transfer than the divider position.

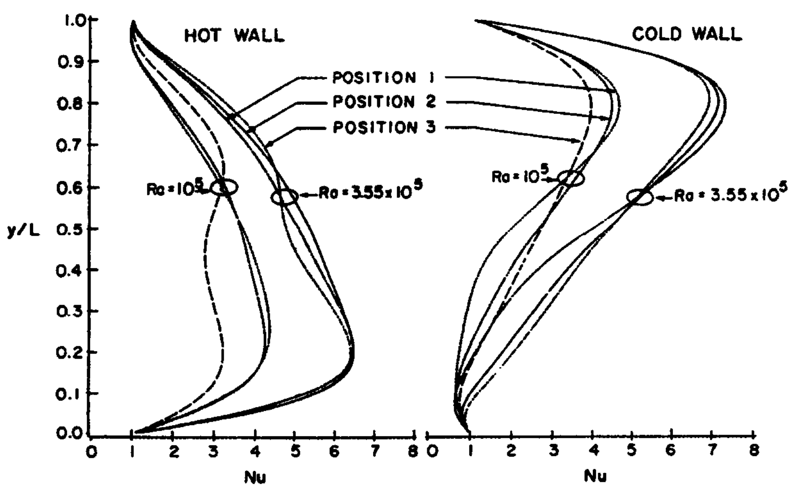

FIG. 9. Local Nusselt numbers along the side walls for the three divider positions ($Ra = 10^5$, 3.55×10^5 and $A_p = 1/2$).

REFERENCES

1. D. Duxbury, An interferometric study of natural convection in enclosed plane air layers with complete and partial central vertical divisions, Ph.D. Thesis, University of Salford, U.K. (1979).
2. K. H. Winters, The effect of conducting division on the natural convection of air in a rectangular cavity with heated side walls, ASME Paper No. 82-HT-69 (1982).
3. M. W. Nansteel, Natural convection in enclosures, Ph.D. Thesis, Department of Mechanical Engineering, University of California, Berkeley, California (1982).
4. M. W. Nansteel and R. Greif, An investigation of natural convection in enclosures with two- and three-dimensional partitions, *Int. J. Heat Mass Transfer* **27**, 561–571 (1986).
5. N. N. Lin and A. Bejan, Natural convection in a partially divided enclosure, *Int. J. Heat Mass Transfer* **26**, 1867–1878 (1983).
6. K. H. Winters, Laminar natural convection in a partially divided rectangular cavity at high Rayleigh number, Harwell Report AERE TRP.1118, Harwell (1985).
7. A. T. Kirkpatrick, M. D. White and C. B. Winn, Numerical study of high Rayleigh number natural convection flows in partitioned enclosures, *Proc. 2nd ASME/JSME Thermal Engng Joint Conf.*, pp. 327–334 (1987).
8. E. Zimmerman and S. Acharya, Natural convection in an enclosure with a vertical baffle, *Commun. Appl. Numer. Meth.* **4**, 631–638 (1988).
9. S. D. Probert and J. Ward, Improvements in the thermal resistance of vertical, air-filled, enclosed cavities, *Proc. Fifth Int. Heat Transfer Conf.*, Tokyo, pp. 124–128 (1979).
10. H. E. Janikowski, J. Ward and S. D. Probert, Free convection in vertical, air filled rectangular cavities fitted with baffles, *Proc. Sixth Int. Heat Transfer Conf.*, Toronto, Vol. 6, pp. 257–263 (1978).
11. S. M. Bajorek and J. R. Lloyd, Experimental investigation of natural convection in partitioned enclosures, *J. Heat Transfer* **104**, 527–532 (1982).
12. L. C. Chang, Finite difference analysis of radiation–convection interactions in two-dimensional enclosures, Ph.D. Thesis, Department of Mechanical and Aerospace Engineering, University of Notre Dame, South Bend, Indiana (1981).
13. E. Zimmerman and S. Acharya, Free convection heat transfer in a partially divided vertical enclosure with conducting end walls, *Int. J. Heat Mass Transfer* **30**, 319–331 (1987).
14. R. Jetli, S. Acharya and E. Zimmerman, The influence of baffle location on natural convection in a partially divided enclosure, *Numer. Heat Transfer* **10**, 521–536 (1986).
15. R. Jetli and S. Acharya, End wall effects on thermal stratification and heat transfer in a vertical enclosure with offset partitions, *Can. J. Chem. Engng* **66**, 563–571 (1988).
16. R. Jetli, Natural convection in enclosures with offset baffles, M.S. Thesis, Louisiana State University, Baton Rouge, Louisiana (1988).
17. R. J. Krane and J. Jesse, Some detailed field measurements for a natural convection flow in a vertical square enclosure, *ASME/JSME Thermal Engng Joint Conf.*, Vol. 1, pp. 323–329 (1983).
18. S. M. El Sherbiny, K. G. T. Hollands and G. D. Raithby, Effect of thermal boundary conditions on natural convection in vertical and inclined air layers, *J. Heat Transfer* **104**, 515–520 (1982).
19. S. J. M. Linthorst, W. M. M. Schinkel and C. J. Hoogendorn, The stratification in natural convection in vertical enclosures. In *Natural Convection in Enclosures* (Edited by K. E. Torrance and I. Catton), ASME HTD Vol. 8, pp. 31–38 (1980).
20. E. Zimmerman and S. Acharya, Natural convection in a vertical square enclosure with perfectly conducting end walls, ASME Solar Energy Conf., Anaheim, California, SED-8, pp. 57–65 (1986).
21. S. V. Patankar, *Numerical Heat Transfer and Fluid Flow*. Hemisphere, New York (1980).
22. S. V. Patankar, A numerical method for conduction in composite materials, flow in irregular geometries and conjugate heat transfer, *Proc. Sixth Int. Heat Transfer Conf.*, Toronto, Vol. 3, pp. 297–302 (1978).

TRANSFERT THERMIQUE DU A LA PESANTEUR DANS UNE BOITE CARREE PARTIELLEMENT DIVISEE

Résumé—On étudie numériquement le transfert de chaleur et les configurations d'écoulement dans une boite carrée divisée partiellement. La cloison est mince, faiblement conductrice et elle renvoie vers le haut, à partir du plancher de la cavité. On considère trois positions de la cloison et plusieurs hauteurs. Des résultats obtenus sont comparés à des études numériques et expérimentales déja publiées: ils fournissent une représentation unifiée de l'écoulement et du transfert thermique dans des cavités partiellement divisées. La stratification thermique entre la cloison et la paroi froide joue un rôle principal. Aux faibles nombres de Rayleigh (10^5–10^6), l'écoulement est faible dans cette région stratifiée et on note une tendance à une séparation de l'écoulement derrière la cloison. Aux plus grands nombres de Rayleigh ($>10^9$), la stratification est marquée dans cette région et elle est la cause du détachement de l'écoulement à partir de la paroi froide, ce qui provoque la séparation devant la cloison. Le transfert thermique est fortement influencé par le rapport d'ouverture A_p ($Nu \simeq A_p^{0.462}$). Néanmoins la position de la cloison a un effet plutôt faible sur le transfert thermique global.

WÄRMEÜBERGANG BEI NATÜRLICHER KONVEKTION IN EINEM TEILWEISE UNTERTEILTEN QUADER

Zusammenfassung—Wärmeübergang und Strömungsformen in einem teilweise unterteilten Quader wurden numerisch berechnet. Die Trennfläche ist dünn, schlecht wärmeleitend und verläuft vom Boden des Hohlraums nach oben. Drei verschiedene Positionen und drei verschiedene Höhen der Trennfläche (Apertur des Hohlraums) werden betrachtet. Die Ergebnisse werden mit veröffentlichten Rechen- und Versuchsergebnissen verglichen und zeigen ein einheitliches Bild von Strömung und Wärmeübergang in teilweise unterteilten Hohlräumen. Die Temperaturschichtung zwischen kalter Wand und Trennfläche spielt eine zentrale Rolle. Bei niedrigen Rayleigh-Zahlen ($\sim 10^5$–10^6) ist die Strömung in diesem Bereich schwach ausgeprägt, und es zeigt sich eine Neigung zur Strömungsablösung hinter der Trennfläche. Bei hohen Rayleigh-Zahlen ($>10^9$) ist die Temperaturschichtung in diesem Bereich erheblich und führt zur Strömungsablösung an der kalten Wand, was dann auch eine Ablösung von der Trennfläche nach sich zieht. Der Wärmeübergang im Hohlraum wird stark vom Aperturverhältnis A_p ($Nu \approx A_p^{0.462}$) beeinflußt. Dagegen hat die Position der Trennfläche nur einen geringen Einfluß auf den Wärmeübergang im Hohlraum.

ТЕПЛОПЕРЕНОС В ЧАСТИЧНО ПЕРЕГОРОЖЕННОЙ КАМЕРЕ КВАДРАТНОГО СЕЧЕНИЯ

Аннотация—Численно исследуются теплоперенос и течение в частично перегороженной камере квадратного сечения. Перегородка является тонкой, плохо проводящей и направленной вверх от основания камеры. Рассматриваются три случая расположения и высоты перегородки (сечений камеры). Полученные результаты сравниваются с данными опубликованных численных и экспериментальных исследований и дают обобщающуюмю картину течения и теплопереноса в частично перегороженных полостях. Найдено, что основную роль играет тепловая стратификация между перегородкой и холодной стенкой. При низких значениях числа Рэлея (10^5–10^6) течение в данной стратифицированной области является слабым, и наблюдается тенденция к отрыву потока за перегородкой. При более высоких значениях числа Рэлея ($>10^9$) стратификация в данной области становится значительной, в результате чето течение отделяется от холодной стенки и перед перегородкой происходит его отрыв. Сильное влияние на теплоперенос в полости оказывает отношение сечений A_p ($Nu \approx A_p^{0.462}$). Однако расположение перегородки незначительно влияет на суммарный теплоперенос от полости.